Levels in ^{221}Fr fed by the α decay of ^{225}Ac

G. Ardisson, J. Gasparro, and V. Barci
Laboratoire de Radiochimie et Radioécologie, Université de Nice, F-06108 Nice Cédex 2, France

R. K. Sheline
Departments of Chemistry and Physics, Florida State University, Tallahassee, Florida 32306

(Received 2 February 2000; published 9 November 2000)

The α decay of ^{225}Ac to ^{221}Fr was reinvestigated by γ-ray spectroscopic studies with HPGe detectors and ^{225}Ac sources purified using continuous elution processes. Energies and intensities of about 120 γ-ray transitions were measured. Among these, 40 are reported for the first time. A ^{221}Fr level scheme with 46 excited states and 124 transitions is proposed. The level structure is described in terms of a reflection asymmetric structure with parity doublet bands $K^{\pi}=1/2^{\pm}$, $3/2^{\pm}$, $5/2^{\pm}$, and $3/2^{\pm}$ in order of increasing energy. Both strong and intermediate coupling models have been shown to be in good agreement with the experimental data.

PACS number(s): 21.10.−k, 21.60.Ev, 23.60.+e, 82.55.+e

I. INTRODUCTION

In nuclei beyond ^{208}Pb with $A\sim219$–227, calculations [1] of the potential energy versus octupole deformation suggest the existence of stable quadrupole-octupole deformations. The barrier height between the mirror minima in the quadrupole-octupole potential energy surfaces determines the stability of the quadrupole-octupole deformed nuclear system. If we consider the odd-A Fr isotopes, this barrier height reaches a maximum of $\sim$1.2 MeV in ^{221}Fr [1].

The α decay of ^{225}Ac leading to ^{221}Fr was studied by Leang [2] and Dzhelepov *et al.* [3,4] using Ge(Li) γ spectrometry and ^{225}Ac sources. Dickens and McConnel [5] used a ^{229}Th source in an equilibrium mixture with daughters. The most recent work was that of Kouassi *et al.* [6–8], who studied the γ-ray spectrum of ^{225}Ac in an equilibrium mixture with daughters and developed a ^{221}Fr level scheme. These data were included by Akovali [9] in her latest Nuclear Data Sheets publication on $A=225$.

As previously suggested [10,11], we have tried here to interpret the ^{221}Fr level scheme as a quadrupole-octupole deformed system, showing parity doublet bands (bands close in energy with the same spins but opposite parities), $K=1/2^{\pm}$ bands with decoupling parameters approaching the same absolute value but opposite sign, and enhanced $E1$ transition rates between members of parity doublet bands.

It has recently become possible to carry somewhat further the analysis of the experimental data on ^{221}Fr following α decay of ^{225}Ac. The source selectivity and the γ-ray sensitivity have been improved by performing a continuous elution [12] of ^{225}Ac daughters, such as ^{221}Fr, ^{217}At, ^{213}Bi, and ^{209}Tl. The remaining contribution of γ rays from the decay of daugther nuclides is known and could be subtracted from the γ-ray spectrum of ^{225}Ac. Also the Compton background resulting from the high-energy γ rays generated towards the end of the α-decay series was reduced.

The objective of this paper is to describe the experimental method used here, present the results, and attempt a further interpretation of the ^{221}Fr level scheme.

II. EXPERIMENTAL METHODS

An initial 2.2 MBq of ^{225}Ac radioactive source was provided to us by SUBATEC Laboratories (Nantes), where this nuclide is used for α-therapy studies. We tested the source for purity before starting the experiment and found no contaminants from the ^{228}Th decay series.

The source was dissolved in 2 M HCl and set on the top of a cationic exchanger Dowex 50 WX-8 column of 7 cm in

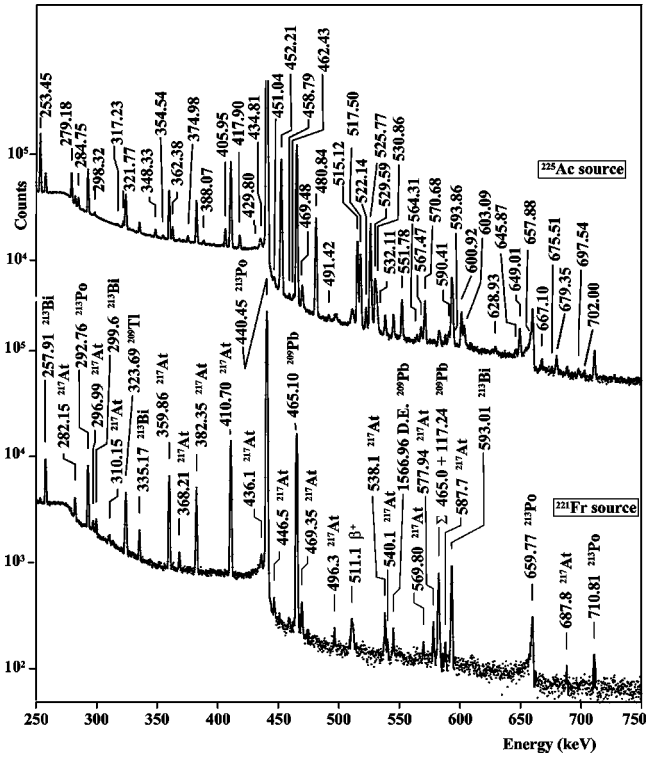

FIG. 1. A ^{225}Ac γ-ray spectrum (measured during a continuous elution of daughter nuclei) compared with a spectrum of a pure ^{221}Fr source showing its daughter components. The transitions that belong to the ^{221}Fr level scheme are labeled at the top spectrum. Those that belong to the daughter nuclei are labeled on the bottom spectrum.

TABLE I. Energies and intensities of γ-ray transitions following the α decay of ^{225}Ac. Uncertainties in the least significant digits are given in parentheses. Unassigned transitions have blank placements; uncertain placements are in parentheses.

This work		Previous work[a]		Placement		
E_γ (keV)	I_γ (%)	E_γ (keV)	I_γ (%)	E_i-E_f(level)	Multipolarity[b]	α[c]
7.5[d]	≈1.0[e]			108.37-100.88	[$M1$]	
10.6[d]	7.8[e] (15)			36.64-26.02	[$M1$]	542
19.0[d]	≈0.04[e]			253.50-234.46	[$M1$]	41.7
26.0 (1)	0.00161 (22)	26.05 (10)		26.02-0	($E2$)	6060
36.70 (3)	0.0183 (23)	36.65 (3)	0.015 (2)	36.65-0	$E2$	1110
38.60 (4)	0.0102 (16)	38.53 (3)	0.011 (1)	38.54-0	$E2$	870
46.24 (5)	0.0057 (12)	46.24 (5)	0.004 (2)	145.84-99.61	[$E1$]	0.86
49.13 (4)	0.0090 (14)	49.09 (5)	0.006 (2)	150.04-100.88	($E1$)	0.727
50.2[d]	≈0.15[e]			150.04-99.84	[$E2$]	241
53.01 (5)	<0.004			(570.69-517.51)	[$M1$]	
57.69 (4)	0.0061 (13)	57.75 (5)	0.004 (2)	253.50-195.75	[$E1$]	0.472
62.6 (3)	0.0053[f] (12)			100.88-38.54	[$E2$]	82.7
62.96 (3)	0.48 (6)	62.95 (5)	0.40 (2)	99.61-36.65	$M1$	11.5
63.5 (3)	0.021 (3)			99.84-36.65	[$E1$]	0.346
64.28 (3)	0.047 (5)	64.28 (5)	0.028 (3)	100.88-36.65	$M1$+21% $E2$	24
69.87 (5)	0.0047 (12)	69.8 (2)	0.005 (2)	108.37-38.54	$E2$	48.7
71.72 (4)	0.0129 (14)	71.74 (3)	0.012 (1)	108.37-36.65	$E2$	43.0
73.36 (20)	0.015 (5)	73.5 (1)	0.008 (2)	99.61-26.02	$E2$	38.6
73.85 (4)	0.32 (4)	73.86 (2)	0.268 (12)	99.84-26.02	$E1$	0.244
74.82 (5)	0.013 (3)	74.9 (2)	0.015 (2)	100.88-26.02	($E2$)	35.2
87.42 (3)	0.31 (4)	87.41 (3)	0.216 (10)	195.75-108.37	$M1$	4.40
94.90 (3)	0.130[g] (19)	94.90 (5)	0.081 (7)	195.75-100.88	$M1$	3.47
96.15 (5)	<0.03	96.15 (5)	0.026 (3)	195.75-99.61	($E2$)	10.8
99.71 (6)	1.36 (19)	99.63 (5)	0.53 (3)	99.61-0	$M1$+3% $E2$	3.22
100.07 (10)	0.26[g] (10)	99.91 (5)	0.86 (5)	99.84-0	$E1$	0.108
100.87 (4)	0.121 (13)	100.96 (5)	0.059 (9)	100.88-0	$M1$+30% $E2$	4.8
103.44 (12)	0.0065 (19)	103.46 (10)	0.004 (2)	253.55-150.04	[$M1$,$E2$]	11
108.38 (3)	0.27 (3)	108.41 (3)	0.21 (1)	108.37-0	$M1$+22% $E2$	10.8
111.52 (3)	0.34 (4)	111.54 (3)	0.269 (12)	150.04-38.54	($E1$)	0.369
112.8 (2)	<0.003	112.8 (2)	0.002 (1)	400.92-288.14	[$E1$]	0.35
119.09 (6)	0.018 (3)					
119.84 (3)	0.097 (10)	119.87 (5)	0.063 (6)	145.84-26.02	[$E1$]	0.310
121.06 (7)	0.017 (5)			271.10-150.04	($E1$)[h]	0.302
123.73 (4)	0.098 (10)	123.75 (5)	0.061 (6)	224.60-100.88	[$E1$]	0.286
124.81 (3)	0.032 (3)	124.82 (5)	0.022 (2)	224.60-99.84	$M1$+39% $E2$	6.3
126.09 (5)	0.0073 (14)	126.15 (10)	0.006 (2)	234.46-108.37	($E1$)	0.273
129.22 (7)	0.0033 (11)	129.2 (2)	0.003 (1)	279.19-150.04	[$M1$,$E2$]	5.2
133.60 (4)	0.096 (19)	133.64 (5)	0.012 (2)	234.46-100.88	($E1$)	0.237
134.85 (3)	0.033 (5)	134.86 (5)	0.026 (3)	234.46-99.61	($E1$)	0.232
137.40 (10)	0.0030 (13)					
144.7[i] (2)	≈0.0005			294.68-150.04	($M1$+40% $E2$)	≈4
145.15 (3)	0.148 (15)	145.17 (5)	0.124 (6)	253.50-108.38	($E1$)	0.194
150.02 (4)	0.691[j] (16)	150.04 (2)	0.68 (3)	150.04-0	$E1$	0.179
152.64 (3)	0.0165 (19)	152.63 (5)	0.015 (2)	253.50-100.88	[$E1$]	0.172
153.91 (3)	0.195 (20)	153.92 (5)	0.159 (7)	253.50-99.61	[$E1$]	0.168
157.24 (3)	0.35 (4)	157.26 (2)	0.31 (2)	195.75-38.54	$M1$+4% $E2$	4.0
161.35 (7)	0.0036 (9)			311.39-150.04	[$M1$,$E2$]	2.6
169.18 (4)	0.0158 (19)	169.1 (2)	0.016 (2)	(517.51-348.33)		
170.83 (6)	0.0073 (13)	170.7 (2)	0.006 (3)	279.19-108.37	($E1$)	0.130

TABLE I. (*Continued*).

This work		Previous work[a]		Placement		
E_γ (keV)	I_γ (%)	E_γ (keV)	I_γ (%)	E_i-E_f(level)	Multipolarity[b]	α[c]
178.29 (3)	0.0160 (18)	178.4 (1)	0.012 (1)	279.19-100.88	$E1$	0.117
179.78 (4)	0.0106 (13)	179.8 (2)	0.006 (2)	288.14-108.37	$(M1,E2)$[h]	1.8
186.31 (3)	0.0189 (21)	186.2 (1)	0.017 (4)	294.68-108.37	$E1$	0.105
187.95 (3)	0.54 (6)	188.00 (5)	0.458 (23)	224.60-36.65	$E1$	0.103
195.74 (3)	0.162 (16)	195.78 (5)	0.14 (1)	195.75-0	$M1+39\%$ $E2$	1.7
197.50 (3)	0.054 (7)	197.7 (1)	0.051 (5)	393.17-195.75	$(E1)$	0.092
198.23[k] (8)		198.7 (1)	0.020 (5)	224.60-26.02		
	0.0176 (18)			234.46-36.65	$[E1]$	0.091
205.12 (11)	0.0019 (7)			458.73-253.50		
216.89 (3)	0.33 (3)	216.90 (5)	0.27 (6)	253.50-36.65	$(E1)$	0.0735
220.43 (8)	0.0060 (18)			320.04-99.61	$(E1)$[h]	0.0705
224.58 (3)	0.108 (12)	224.64 (5)	0.081 (7)	224.60-0	$[E1]$	0.0674
231.14 (7)	0.0021 (5)	231.3 (2)	0.002 (1)	748.85-517.51	$(M1)$[h]	1.41
238.64 (8)	0.0010 (3)			338.25-99.61	$(M1)$[h]	1.29
240.68 (3)	0.0118 (13)	240.8 (1)	0.006 (2)	279.19-38.54	$[E1]$	0.0572
243.11 (5)	0.0027 (5)	243.2 (1)	0.0011 (5)	393.17-150.04	$[M1]$	1.22
249.60 (3)	0.0131 (14)	249.5 (2)	0.010 (5)	288.14-38.54	$(E2)$[h]	0.263
253.45 (3)	0.128 (13)	253.54 (5)	0.105 (5)	253.50-0	$[E1]$	0.0507
256.0 (2)	0.00032[g] (10)			294.65-38.54	$[E1]$	0.0496
279.18 (3)	0.032 (3)	279.25 (10)	0.016 (2)	279.18-0	$E1$	0.0406
284.75 (3)	0.0075 (9)	284.8 (1)	0.004 (2)	393.17-108.37	$[E1]$	0.0388
298.32[k] (5)	0.0020 (3)			406.69-108.37	$(M1,E2)$[h]	0.4
				551.80-253.50		
317.23[k] (18)				551.80-234.46		
	0.00042 (21)			570.70-253.50	$[M1]$	0.588
321.77[k] (4)	0.0032 (5)			422.63-100.88	$[E1]$	0.0294
				517.51-195.75		
348.33 (4)	0.0032 (5)	348.5 (1)	0.003 (1)	348.33-0		
354.54 (6)	0.00128 (23)	354.8 (2)	0.0014 (4)	393.17-38.54	$[E1]$	0.0237
362.38 (3)	0.0062 (7)	362.5 (1)	0.006 (2)	400.92-38.54	$(E1)$[h]	
367.72 (12)	0.00037[f] (19)			367.72-0		
374.98 (5)	0.00019 (3)	375.2 (1)	0.003 (1)	570.70-195.75	$[E1]$	
388.07 (7)	0.00121 (23)			496.44-108.37		
403.1 (1)	$<$0.002	403.1 (1)	0.0012 (4)	637.57-234.46		
405.95 (3)	0.0079 (9)	406.1 (1)	0.007 (2)	551.80-145.84	$[E1]$	
417.90 (3)	0.0057 (7)	418.1 (1)	0.005 (1)	517.51-99.61		
429.80 (18)	0.00038 (19)			852.06-393.17		
434.81 (5)	0.0032 (5)			630.49-195.75		
442.16 (8)	0.0045 (7)			(713.31-271.10)		
443.43[k] (10)	$\approx$0.0001			481.97-38.54		
	0.0014 (5)			551.80-108.37	$[E2]$	0.0500
446.31 (10)	0.0006[g] (3)			446.31-0		
451.04 (5)	0.0028 (5)			551.80-100.88	$[M1]$	0.227
452.21 (3)	0.118 (13)	452.4 (1)	0.100 (8)	551.80-99.84	$[M1]$	0.225
458.79 (8)	0.00045 (11)	458.8 (2)	0.005 (2)	458.73-0		
462.43 (13)	0.00038 (11)	462.4 (4)	0.015 (7)	570.70-108.37	$[E1]$	
469.48 (5)	0.0018[g] (7)	469.5 (3)	0.004 (1)	(570.70-100.88)		
480.84 (3)	0.034 (4)	481.05 (5)	0.028 (3)	517.51-36.65		
491.42 (10)	0.00039 (12)					
515.12 (3)	0.0204 (21)	515.40 (5)	0.017 (2)	551.80-36.54	$[M1]$	0.159
517.50 (3)	0.0145 (15)	517.78 (5)	0.012 (2)	517.51-0		
522.14 (4)	0.00205 (24)	522.3 (1)	0.014 (4)	630.49-108.37		

TABLE I. (*Continued*).

This work		Previous work[a]		Placement		
E_γ (keV)	I_γ (%)	E_γ (keV)	I_γ (%)	E_i-E_f(level)	Multipolarity[b]	α[c]
525.77 (3)	0.032 (3)	526.09 (5)	0.027 (3)	551.80-26.02	[$M1$]	0.151
527.29 (5)	0.0019 (3)					
529.59 (3)	0.0070 (8)	529.9 (1)	0.006 (3)	630.49-100.88		
530.86 (4)	0.0047 (6)	531.3 (1)	0.004 (1)	630.49-99.61		
532.11 (9)	0.00073 (19)			570.70-38.54	[$E1$]	
551.78 (3)	0.0039 (5)	552.0 (1)	0.004 (1)	551.80-0	[$M1$]	0.133
564.31 (11)	$\approx$0.0001[g]			600.92-36.65		
567.47 (5)	0.00093 (13)			713.31-145.84		
570.68 (3)	0.0041 (5)	571.0 (1)	0.004 (1)	570.70-0	[$E1$]	
590.41 (5)	0.00084 (14)					
593.86 (4)	0.0028 (3)	594.2 (1)	0.0015 (7)	630.49-36.65		
600.92[k] (3)	0.0024 (4)	601.1 (1)	0.0031 (9)	600.92-0		
	$\approx$0.006			637.57-36.65		
603.09 (4)	0.00170 (21)	603.3 (1)	0.002 (1)	748.85-145.84		
628.93 (10)	0.00034 (9)			779.19-150.04		
645.87 (13)	0.00022 (7)			645.87-0		
649.01 (4)	0.00185 (22)	649.2 (1)	0.0012 (4)	748.85-99.84		
656.18 (11)	0.00049 (23)			852.03-195.75		
657.88 (5)	0.0014 (3)			766.49-100.88		
667.10 (8)	0.0039 (9)			766.49-99.84		
675.51 (18)	0.00013 (6)			825.55-150.04		
679.35[k] (6)	0.00062 (12)	679.7 (1)	0.008 (2)	679.35-0		
				779.19-99.61		
697.54 (13)	0.00024 (9)					
702.00 (14)	0.00016 (7)			852.06-145.84		
747.0 (1)	$<$0.002	747.0 (1)	0.0011 (4)	942.75-195.75		
752.46 (12)	0.00026 (7)			852.06-99.61		
754.04 (13)	0.00023 (7)	753.7 (3)	0.0008 (2)	779.19-26.02		
767.6 (4)	0.00034 (9)			766.49-0		
808.48 (10)	0.0021 (3)			808.48-0		

[a]From Ref. [8].

[b]Multipolarities and mixing ratios are from Refs. [3,4,23]. Multipolarities in square brackets are from level scheme.

[c]Theoretical values from Hager and Seltzer [24], interpolated with the computer code HSICC.

[d]Not seen in the γ-ray spectrum, but required by coincidence mesurements or intensity balance.

[e]Total $(\gamma+ce)$ intensity from the γ-ray transition intensity balance at the relevant level.

[f]Transition observed with $I_\gamma<0.03$, but intensity calculated assuming identical strength for the two similar ($E2$) interband transitions deexciting the 100.88-keV level $[I_{\gamma1}/I_{\gamma2}=(E_{\gamma1}/E_{\gamma2})^5$ or $I(62.6)/I(74.82)=(62.6/74.82)^5]$.

[g]Multiple transition, spurious components were subtracted.

[h]From γ-ray intensity balance, assuming the level scheme shown in Fig. 2.

[i]Seen in ^{225}Ac α decay, but intensity deduced from ^{221}Rn β decay.

[j]Normalizing transition. Intensity = 0.796(11)% is from Ref. [15], but corrected for a 0.051(10)% component from ^{221}Fr$\rightarrow^{217}$At decay and a 0.054(6)% component from ^{229}Th$\rightarrow^{225}$Ra decay (see Sec. III). These components were subtracted.

[k]Multiply placed transition. Only the strongest transition is given, or the intensities are suitably divided.

length and 3 mm in diameter connected by means of a peristaltic pump to a 2 M HCl reservoir. The top of the column was centered in front of a HPGe detector through a 5 mm hole in a lead sheet 10 mm thick. To reduce background the source and the detector were set inside a 50-mm-thick lead castle with a 5-mm-thick copper lining.

We used a 17% efficiency coaxial HPGe detector with an energy resolution [full width at half maximum (FWHM)] of 1.9 keV at 1333 keV (^{60}Co); low-energy γ-ray spectra were measured with a 2-cm^2 HPGe planar detector with a resolution (FWHM) of 210 eV for the Fe $K\alpha\ x$ line. These detectors were calibrated for energy and intensity using multi-γ

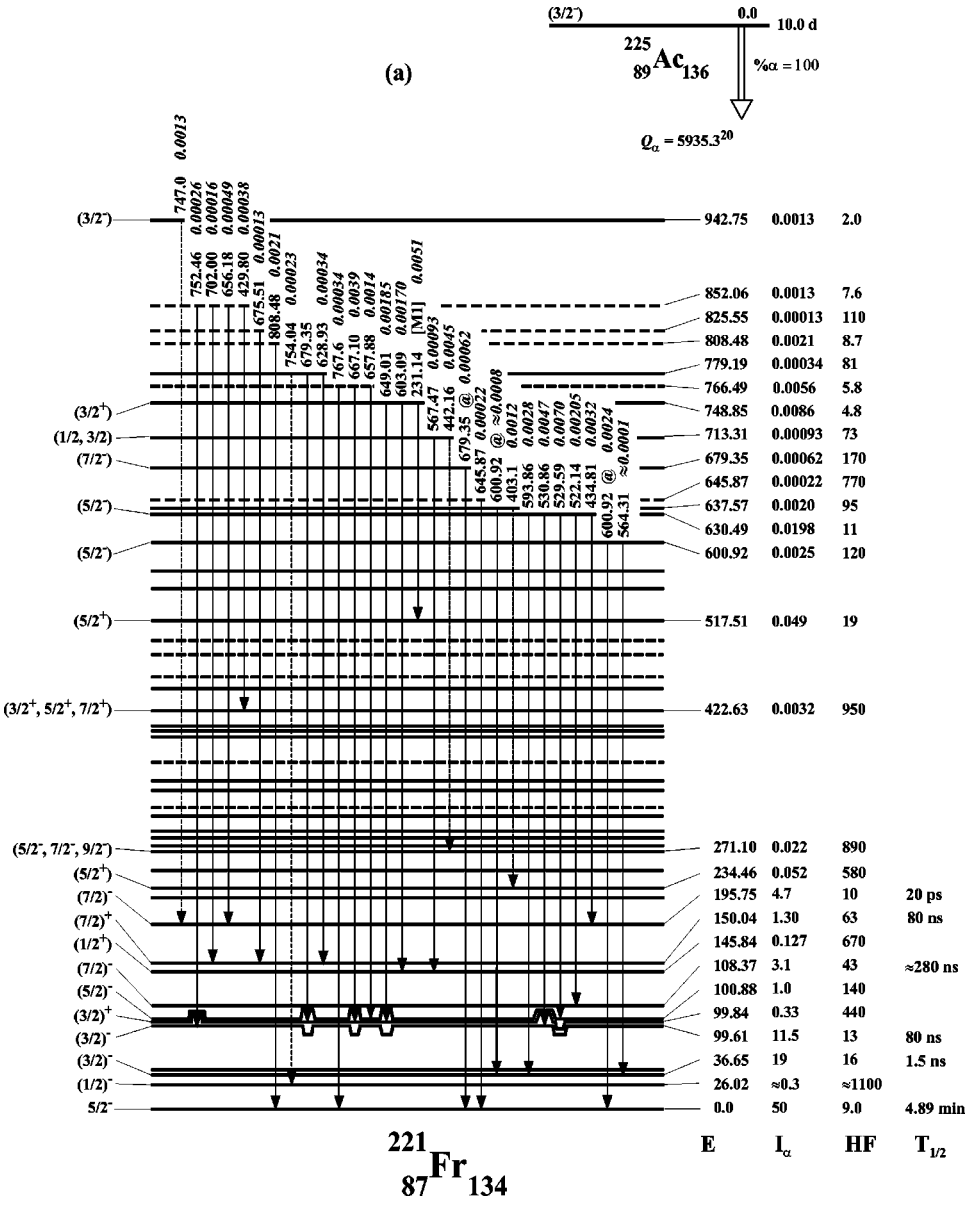

FIG. 2. ^{225}Ac α-decay scheme. Energies values in keV are rounded to two or fewer decimal digits; @ denotes γ transitions placed twice; dotted γ rays are uncertain. Multipolarities are from Refs. [3,4,23]; those in parentheses are uncertain, and those in squared brackets have been deduced from the level scheme. Transition intensities are total ($\gamma + ce$) per 100 decays of the parent nuclide. Alpha intensities are from Refs. [21,14,22]; half-lives are from Refs. [11,20].

standard sources such as ^{152}Eu, ^{207}Bi, ^{133}Ba, and ^{137}Cs; for low-energy spectra ^{241}Am and ^{133}Ba sources were used. Single γ-ray spectra were recorded on 8192-channel analyzers.

The γ-ray spectrum of ^{225}Ac was measured with the coaxial HPGe detector while continually eluting the daughter products, mainly ^{221}Fr, ^{213}Bi, and ^{209}Tl. The elution rate 0.15 mL/min was chosen as a compromise to discard ^{221}Fr ($T_{1/2}$=4.9 min) faster than ^{225}Ac. Spectra were recorded every hour to check the efficiency of the purification by determining the intensity ratio from the main photopeaks of ^{221}Fr (218 keV), ^{213}Bi (440 keV), ^{209}Tl (465 keV), and ^{225}Ac (188 keV).

In some experiments the ^{225}Ac source was counted with lead and copper sheets (1 and 5 mm thick, respectively) inserted between source and detector in order to absorb low-energy γ rays, thus enhancing the count rate of high-energy γ rays. The ^{225}Ac was eluted of the column after $\sim$14 h. Here ^{225}Ac was then completely desorbed using 10 M HCl solution, taken to dryness, dissolved in 2M HCl, and recycled to the top of the column.

III. RESULTS

The γ-ray data were analyzed with the computer code GAMANAL [13]. Figure 1 shows part of the γ-ray spectrum of a pure ^{225}Ac α source, counted for 26 h. As a result of α-particle recoil and the short half-lives of the daughter products, these remained implanted in the resin grains and the decontamination factors reached a limit of $\sim$10, $\sim$13, and $\sim$2 for ^{213}Bi, ^{209}Tl, and ^{221}Fr, respectively. Consequently we had an incomplete separation of the daughter radionuclides and therefore we had to carry out an analysis with a pure ^{221}Fr source, whose γ-ray spectrum is also shown in Fig. 1. The contributions of the daugther radionuclides were clearly identified and could be subtracted from the ^{225}Ac γ-ray spectrum using the data of Refs. [12,14].

The normalization to absolute intensities per 100 decays

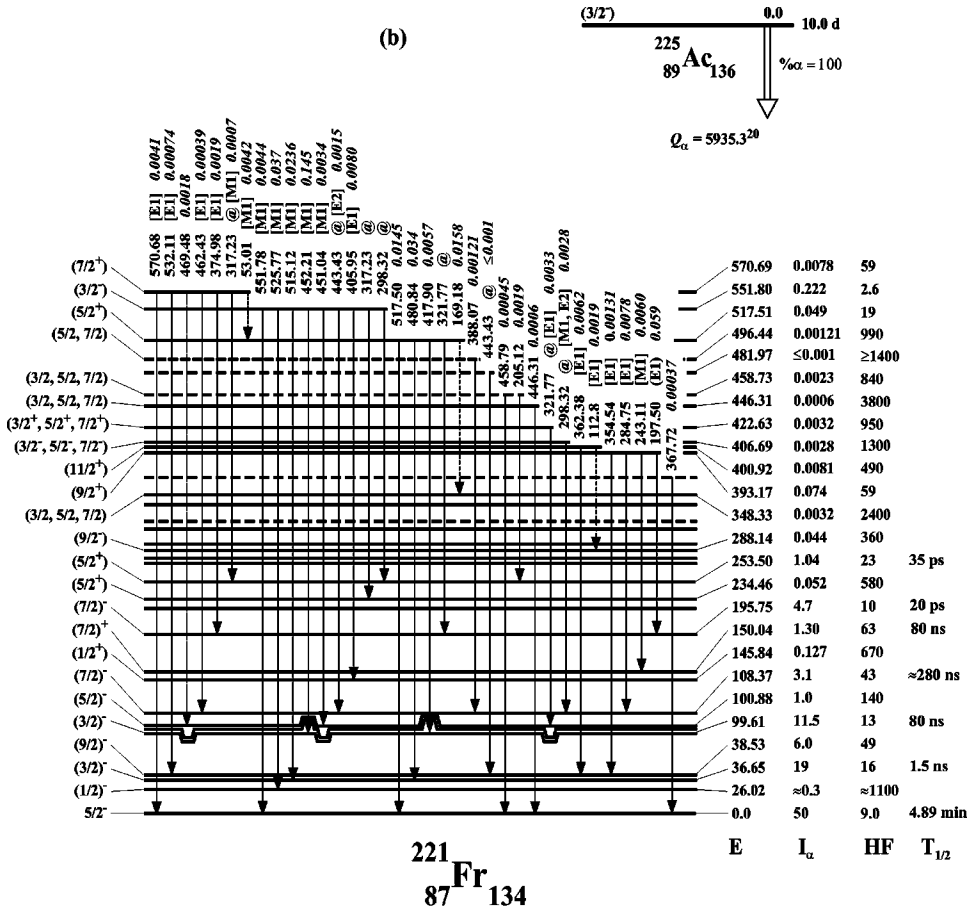

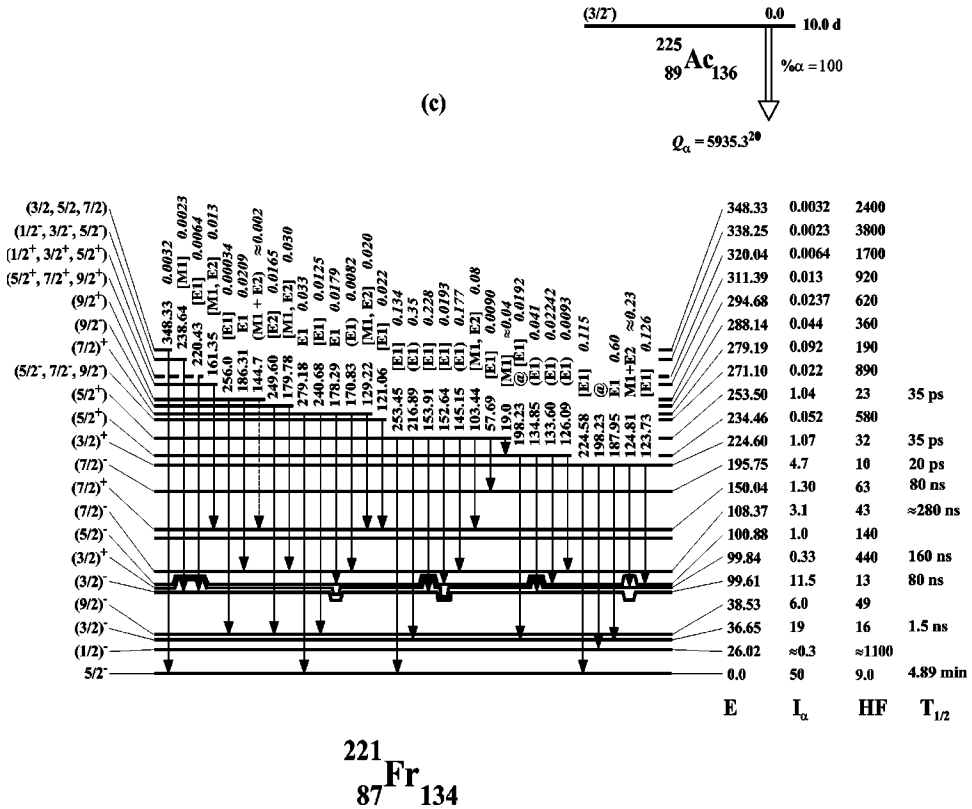

FIG. 2. (*Continued*).

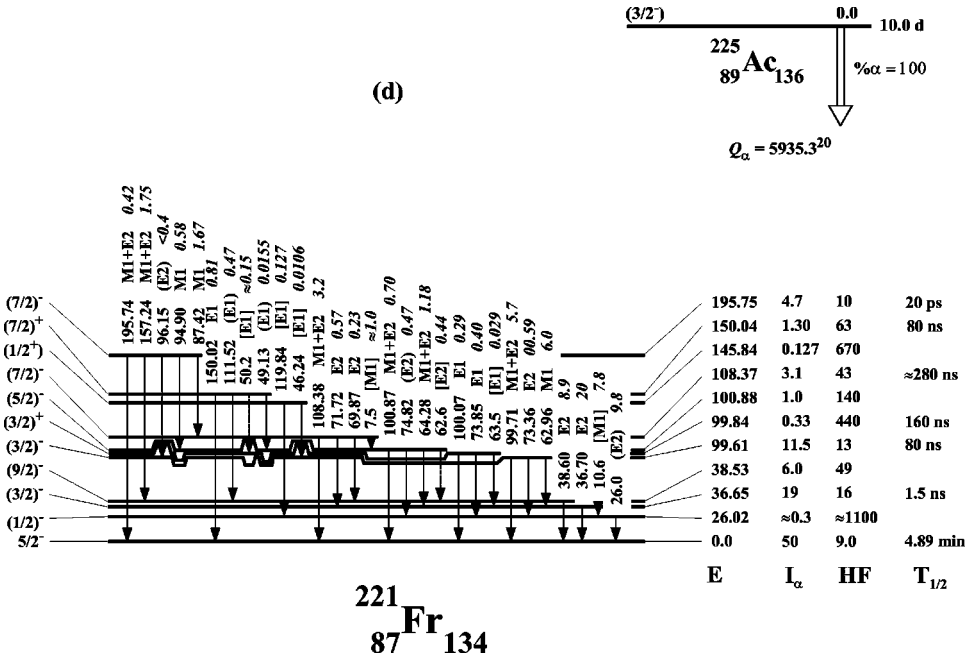

FIG. 2. (*Continued*).

of the parent was carefully done. The intensity of the 150.0-keV γ transition is usually taken as in Ref. [9]; it was best measured in the 1980s by Helmer *et al.* [15], $I_\gamma = 0.796(11)$ per 100 decays, using a ^{229}Th source in equilibrium with its daughters. We know now that there are weak contributions of 0.051(10)% [14] [recently reported also by Sheline *et al.* [16], 150.1(1) keV, 0.060(10)%] from a 150.14(10)-keV transition from ^{221}Fr α decay and a 0.054(6)% [17] [see also Ref. [18], 150.04(2) keV, $<0.06\%$] from a 149.89(10)-keV transition from ^{229}Th α decay. The best intensity of the 150.02(4)-keV transition after subtracting these contributions is therefore 0.691(16)%. A recent paper by Chumin *et al.* [19], who measured the α-particle spectrum in coincidence with a gate at $\sim$150 keV in the γ-ray spectrum of a ^{225}Ac source, also supports our analysis. They found three α groups at 5682, 5980, and 6610 keV in the ratios 870(20)/61(2)/1.0(1), which certainly must be assigned to ^{225}Ac, ^{221}Fr, and ^{221}Ra. This measurement allowed an independent determination of the intensity of the 150-keV transition from ^{225}Ac decay, i.e., 0.693(12)%, in good agreement with our value. A further remark must be given: the values of Ref. [8] were inaccurately normalized by Akovali [9] in Nuclear Data Sheets (off by a factor of 1.09) using a value of 0.796% for the 150-keV γ ray now definetively known to be a multiplet. The best normalization is off by a factor of 0.926, the ratio of Helmer's reference value (11.57%) for the 218-keV transition in ^{217}At in transient equilibrium, to the previous value of 12.5%, used instead by Goffi-Kouassi [8].

Table I summarizes the results of the present work compared to those of the previous study of Goffi-Kouassi [8], cited in Nuclear Data Sheets [9]. Our results are in good agreement with theirs. 40 out of the 120 γ rays reported here are newly found, and were detected by use of the continuous elution process. Some γ-ray lines previously reported in [6] have been now assigned to ^{221}Fr α decay using an improved measurement of its γ-ray spectrum with separated sources [14]. Furthermore, the 758.9-keV γ-ray transition has been assigned to the ^{217}At α decay now.

IV. ^{221}Fr LEVEL SCHEME

The ^{221}Fr level scheme was built primarily using the data presented here, on the basis of Ritz's combination principle, since there are no data from nuclear reactions leading to ^{221}Fr nuclear states.

To complete the level scheme and deduce intensity balances at each level we have taken into account the γ-γ coincidence results reported in our previous papers [6–8], the α-γ coincidence data [20], the experimental singles α-particle data [21,22], the conversion-electron data [3,4], and the β-decay data [23].

Calculations were carried out with the program package of the ENSDF (Evaluated Nuclear Structure Data Files) program library provided by the NNDC (National Nuclear Data Center, Brookhaven). We used the code GTOL, to deduce level energies from a least-squares fit to γ-ray energies; HSICC, to interpolate theoretical conversion coefficients [24] for various γ-ray energies, and ALPHAD, to calculate α-particle hindrance factors.

The ^{221}Fr level scheme proposed here is shown in Fig. 2. The spins and parities of the levels were assigned assuming $E1$, $M1$, and $E2$ multipolarities for the observed γ-ray transitions. Definite assignments could not be given for many levels, for which we are giving our ''best'' assignments based on theoretical arguments reported below (Sec. V). Theoretical calculations have allowed a consistent interpretation of the level scheme, but some experimental data need further discussion because of remaining discrepancies, especially with the β-decay data of Ref. [23].

Vylov *et al.* [23] assigned an $M1+E2$ multipolarity to the 74.82-keV transition, between the 100.8- and the 26.0-keV levels, from a measured L-conversion coefficient of ~ 10 $[I_{e^-}(\Sigma L)/I_\gamma = \sim 1.5/\sim 0.15$, where the theoretical coef-

ficients [24] are $\alpha_L(M1)=5.2$, $\alpha_L(E2)=25.7$] instead of $E2$, as we have assumed. From our measured value of $I_\gamma(73.48)/I_\gamma(64.28)=0.28(7)$ and $I_\gamma(64.28)=0.26(2)$ from Ref. [23], however, one obtains $\alpha(L)=\sim 1.5/0.072(18)=\sim 21$. This result suggsets a pure $E2$ multipolarity for the 73.48-keV γ ray, consistent with $I^\pi=1/2^-$ for the 26-keV level. Moreover, this assignment is in better agreement with the high α-hindrance factor of ~ 1100 to the 26-keV level; since the parent configuration has $K=3/2$, the favored α-particle transitions should involve states with an appreciable contribution of this configuration, and mixing is not possible for spin $I=1/2$.

Values of $\log ft$'s, incompatible with our spin assignments, for the β transitions to the 99.61- and 99.84-keV levels (7.5 and 7.1, respectively) in the ^{221}Rn decay were proposed by Vylov *et al.* [23]. If the intensities of the transitions deexciting these two levels were calculated using our γ-ray intensities and assuming a different decomposition of the multiplets at ~ 63 keV and at ~ 100 keV, their β feedings would be strongly reduced. The $\log ft$ value of the transition to the 99.61-keV level would increase up to 8.5, in better agreement with a possible first-forbidden unique β transition ($\log f^{1u}t \approx 9.0$). For the 99.84-keV level a possible explanation is a missing transition: a 50.2-keV transition, 150.0→99.8, probably $E2$, highly converted [theoretical $\alpha(E2)=241$ [24]], was suggested by Péghaire [20] from α-γ coincidence measurements, with $I_{total}=\sim 0.1$ [~ 0.15 from intensity imbalance at the level, to account for the experimental α and $(\gamma+ce)$ feedings]. Its conversion electrons may be masked by strong lines from other transitions (L lines by M lines from the 36.6-keV transition and M lines by L lines from the 64.28-keV transition). The resulting β feeding may be negligible.

Finally, a weak 96.15-keV transition, 195.75→99.61, was not observed in the γ-ray spectrum, and is probably strongly masked by $K\beta_3$ Fr x rays. We assumed an $E2$ character for this γ ray instead of $M1+E2$ as suggested by Dzhelepov *et al.* [3,4] from the observation of L-conversion lines. A new conversion electron measurement would be helpful to clarify the matter.

The α intensities were calculated from the total $(\gamma+ce)$ intensity imbalances at each level (Table II). They have been found in reasonable agreement with measured values [21,22]. Owing to the ambiguity of the multipolarity assignments, the deduced α feedings of low-energy levels have larger uncertainties. Hindrance factors were calculated using Preston's [25] spin-independent equations (code ALPHAD).

We discuss here only properties of levels for which major changes have been made to the existing decay scheme. All the levels previously known only from α-particle data have been also identified here by their γ rays. Level assignments have been based on the existence of γ-ray transitions fitting the experimental α-particle energies and intensities. New levels at 766.5 keV (deexcited by three γ-ray transitions) and at 852.5 keV (deexcited by four γ-ray transitions) have been proposed here; their corresponding α-particle branches are very weak and may have not been detected.

The 271.1-keV level, populated by an α-particle group

TABLE II. Experimental α-particle abundances compared to values deduced from γ-ray transition intensity balances.

E_{level}[a] (keV)	Alpha-particle abundances This work[b]	Previous works[c]	Hindrance factors
0.0	50 (4)	50.7 (15)	9.0
26.016 (23)	0.3 (21)	0.3	≈1100
36.647 (14)	19 (4)	18.1 (20)	16
38.534 (17)	6.0 (15)	8.6 (9)	49
99.609 (16)	11.5 (12)	8.0 (1)	13
99.84 (3)	0.33 (13)	1.32 (10)	440
100.878 (14)	1.0 (4)	0.87 (23)	140
108.371 (15)	3.1 (5)	3.1 (5)	43
145.836 (24)	0.127 (14)		670
150.038 (21)	1.30 (11)	1.3 (2)	63
195.751 (15)	4.7 (4)	4.4 (3)	10
224.602 (19)	1.07 (8)	1.1 (1)	32
234.464 (24)	0.052 (8)	0.04	580
253.502 (15)	1.04 (6)	1.2 (1)	23
271.10 (8)	0.022 (7)	0.034	890
279.192 (19)	0.092 (11)	0.1	190
288.14 (3)	0.044 (12)	0.03 (1)	360
294.68 (4)	0.0237 (24)	0.015	620
311.39 (8)	0.013 (6)	0.007 (3)	920
320.04 (9)	0.0064 (20)	≈0.005	1700
338.25 (9)	0.0023 (7)	≤0.003	3800
348.33 (4)	0.0032 (5)	0.020 (7)	2400
367.72 (12)	0.00037 (19)	≤0.001	16000
393.170 (22)	0.074 (8)	0.14 (1)	59
400.92 (4)	0.0081 (13)	0.07 (2)	490
406.69 (6)	0.0028 (8)	≤0.003	1300
422.63 (5)	0.0032 (6)	0.0020 (5)	950
446.31 (10)	0.0006 (3)	0.0010 (5)	3800
458.73 (7)	0.0023 (7)	≤0.001	840
481.97 (11)	≤0.001	≤0.001	>1400
496.44 (8)	0.00121 (23)	≤0.001	990
517.513 (18)	0.049 (5)	0.07 (1)	19
551.798 (17)	0.222 (17)	0.23 (1)	2.6
570.695 (25)	0.0078 (8)	0.014 (5)	59
600.92 (3)	0.0025 (4)	0.0030 (8)	120
630.495 (20)	0.0198 (12)	0.030 (3)	11
637.57 (4)	0.0020 (4)	0.0020 (5)	95
645.87 (13)	0.00022 (7)	≤0.002	770
679.35 (6)	0.00062 (12)	0.0020 (8)	170
713.31 (6)	0.00093 (13)	0.0020 (8)	73
748.85 (4)	0.0086 (13)	0.006 (1)	4.8
766.49 (13)	0.0056 (10)		5.8
779.19 (6)	0.00034 (9)	0.003 (1)	81
808.48 (10)	0.0021 (3)	≤0.001	8.7
825.55 (19)	0.00013 (7)	≤0.001	110
852.06 (7)	0.0013 (4)		7.8
942.75 (11)	0.0013 (5)	0.0020 (5)	2.0

[a]Fitted to γ-ray transition energies with the computer code GTOL.
[b]From γ-ray transition intensity balance.
[c]From Ref. [9]: weighted average of measured α-particle abundances from Refs. [21,22].

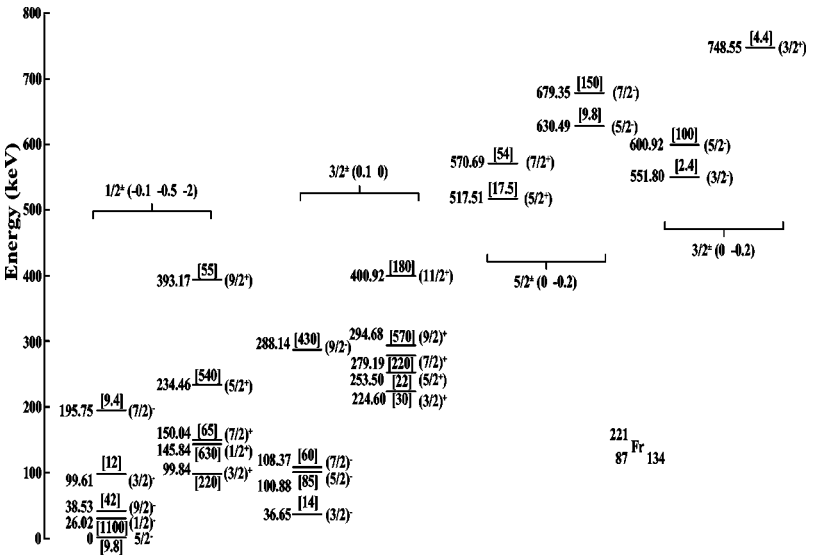

FIG. 3. ^{221}Fr energy levels from Fig. 2, displayed as parity doublet bands. The quadrupole-octupole configurations given here between brackets above and below the appropriate sets of parity doublet bands are from Fig. 4.

with $E_\alpha = 5563$ keV, $I_\alpha = 0.034\%$, and deexcited by a 121.06-keV γ-ray transition ($I_\gamma = 0.017$), has been proposed here. This level replaces the 273.5-keV level that was based on a 273.5-keV transition, not observed in our spectrum.

Other possible levels at 311.4, 320.0, and 338.3 keV have been proposed here with deexciting transitions of 161.35 keV ($I_\gamma = 0.0036$), 220.43 keV ($I_\gamma = 0.0060$), and 238.64 keV ($I_\gamma = 0.0010$), respectively, and populated by α-particle groups of 5525 keV ($I_\alpha = 0.007\%$), 5517 keV ($I_\alpha \approx 0.005\%$), and 5497 keV ($I_\alpha < 0.003\%$).

The 348.8-keV level has been confirmed, with a deexciting γ-ray transition [$I_\gamma = 0.0032(5)$] to the ground state and populated by an α-particle group of 5489 keV [$I_\alpha = 0.0020(7)\%$].

The deexcitation of the 393.2-keV level partially disagrees with previous measurements. The energy of the 169.18-keV γ-ray transition was measured with greater accuracy and consequently could not be placed from this level. Low-intensity transitions (98.8, 105.0, 114.0, and 139.6 keV) suggested by Péghaire [20] from α-γ coincidences were not observed here, possibly because they were under our detection limit. Some γ-ray intensity may be missing because the experimental intensity imbalance is 0.074(8)%, whereas the measured α-particle feeding is 0.14(1)%.

Finally we have proposed some tentative deexciting γ-ray transitions for the 367.7, 406.7, 422.6, 446.3, 458.7, 482.0, 496.4, 645.9, 713.3, 808.5, and 825.1-keV levels, previously known from α-particle singles spectra.

V. DISCUSSION AND COMPARISON WITH THEORY

In Fig. 3 the levels of ^{221}Fr from Fig. 2 are organized so as to emphasize the existence of parity doublet bands, as originally suggested in Refs. [10,11]. Here the band and parity doublet structures are carried somewhat further. This approach in turn suggests that the nuclear structure we are dealing with in ^{221}Fr involves quadrupole-octupole deformation, either static or dynamic.

For a static octupole deformation the coupling between collective octupole modes and single quasiparticle degrees of freedom has been assumed to be strong. The resulting average nuclear field acquires a stable reflection asymmetric deformation, often referred to as strong coupling, by introducing *a priori* a given deformed field with stable octupole deformation. In the example presented here a folded Yukawa field [1] has been used. The resulting level diagram for single proton orbitals is shown in Fig. 4. It has been calculated for an axially symmetric reflection asymmetric folded Yukawa

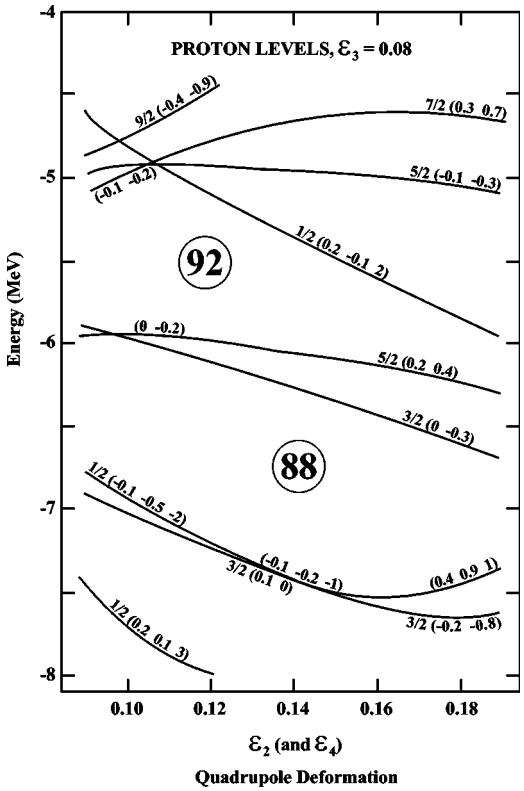

FIG. 4. Energies of single proton orbitals in an axially symmetric but reflection asymmetric folded Yukawa potential with $\epsilon_3 = 0.08$ plotted against the quadrupole deformation (ϵ_2). The orbitals are labeled by Ω and, in parentheses, by a set of single-particle matrix elements (see text). Proton numbers are shown in circles.

potential with an octupole deformation of $\epsilon_3 = 0.08$, and plotted against a quadrupole deformation ϵ_2. The orbitals in Fig. 4 are labeled by Ω and, in parentheses, by the single particle matrix elements $\langle \hat{s}_z \rangle$, $\langle \hat{\pi} \rangle$, and for $K = 1/2$ bands by $\langle \hat{\pi}_{conj} | -\hat{J}_+ | \hat{R}_{conj} \rangle$.

The levels in Fig. 3 have been interpreted in terms of $K^\pi = 1/2^\pm$, $K^\pi = 3/2^\pm$, $K^\pi = 5/2^\pm$, and $K^\pi = 3/2^\pm$ parity doublet bands with a known quadrupole deformation $\epsilon_2 = 0.12$ [10]. This interpretation follows directly from the level structure of Fig. 4. The ground state of ^{221}Fr (with 87 protons) is expected (Fig. 4) to be the observed parity doublet $K^\pi = 1/2^\pm$ arising from the configuration $1/2(-0.1, -0.5, 2)$. Figure 4 suggests that the hole configuration 3/2(0.1,0) gives rise to $K^\pi = 3/2^\pm$ parity doublet bands almost degenerate with the ground state. Considerably above these configurations, the mixed $5/2(0, -0.2)$ configurations and the $3/2(0, -0.3)$ configuration are both expected to give rise to $K^\pi = 5/2^\pm$ and $3/2^\pm$ parity doublet bands. Thus, not only the presence of $K^\pi = 1/2^\pm$, $3/2^\pm$, $5/2^\pm$, and $3/2^\pm$ parity doublet bands, but also their energy ordering is being predicted by our calculations (Fig. 4). The $K^\pi = 1/2^\pm$ parity doublet bands in ^{221}Fr have large decoupling parameters of 4.3 and -2.6, similar in absolute magnitude but opposite in sign, as expected for a reflection asymmetric nucleus. Thus the strong coupling model [1] gives a very satisfactory description of the levels in ^{221}Fr.

In the alternative model, often described in the literature as intermediate coupling, or in the quasiparticle plus phonon model, it is possible to obtain a more quantitative comparison between experiment and theory. In this model a standard reflection asymmetric form is assumed for the average nuclear field and the coupling between the octupole and quasiparticle modes is treated as a residual interaction. Thus there is no octupole deformation, but the effect of very-low-lying octupole vibrations in the neighboring even-even nuclei induces large octupole phonon admixtures in the low-lying states of odd-A nuclei.

In Fig. 5 the experimental level structure of Fig. 3 is compared with the theoretical levels of ^{221}Fr calculated in Ref. [26]. Details of the calculation and a table of the calculated structural configurations of the intrinsic states are given in Ref. [26]. In general, the agreement is satisfactory, particularly with the anomalous structures of the $K^\pi = 1/2^\pm$ bands, which are well reproduced. The experimental values of 4.3 and -2.6 for the decoupling parameters may be compared with theoretical estimates of 3.5 and -2.3 for the $K^\pi = 1/2^-$ and $K^\pi = 1/2^+$ bands, respectively.

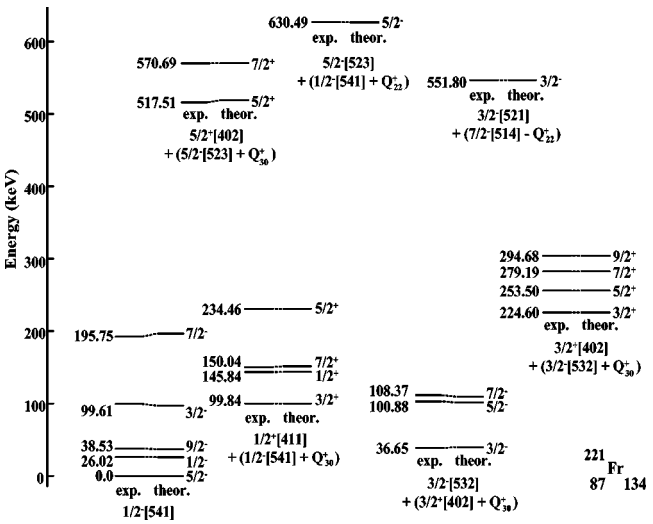

FIG. 5. Band structure in the reflection asymmetric nucleus ^{221}Fr. The experimental energies are shown on the left of each set connected by a dotted line to the theoretical levels on the right. The theoretical level energies were calculated using the intermediate coupling of the appropriate reflection symmetric quasiparticles and octupole degrees of freedom. Major configurations are given under each band.

VI. CONCLUSIONS

The level structure of ^{221}Fr has been extended by a reinvestigation of the γ rays following the α decay of ^{225}Ac and using a continuous chemical elution process which allowed a more complete γ-ray spectrum to be observed. The resulting ^{221}Fr level structure has been interpreted in terms of a series of parity doublet bands which follow directly from a strong coupling model that involves stable octupole deformation. An intermediate coupling model (the quasiparticle plus phonon model) also produced results which agreed remarkably well with experimental level energies.

ACKNOWLEDGMENTS

It is a pleasure to thank Philippe Abela for technical assistance. Thanks are also due to Dr. Jean Charles Abbé who provided us with the ^{225}Ac source. One of us (R.K.S.) also thanks the Florida State University for support.

[1] G.A. Leander and R.K. Sheline, Nucl. Phys. **A413**, 375 (1984).
[2] C.F. Leang, C. R. Acad. Sci., Ser. B **265**, 417 (1967).
[3] B.S. Dzhelepov, A.V. Zolotavin, R.B. Ivanov, M.A. Mihkailova, V.O. Sergeev, and M.I. Sovtsov, Bull. Acad. Sci. USSR, Phys. Ser. **34**, 1897 (1971).
[4] B.S. Dzhelepov, R.B. Ivanov, M.A. Mihkailova, and V.O. Sergeev, Bull. Acad. Sci. USSR, Phys. Ser. **36**, 1832 (1973).
[5] J.K. Dickens and J.W. McConnel, Radiochem. Radioanal. Lett. **47**, 331 (1981).
[6] M.C. Kouassi, J. Dalmasso, H. Maria, G. Ardisson, and M. Hussonnois, J. Radioanal. Nucl. Chem. **144**, 387 (1990).
[7] M.C. Kouassi, J. Dalmasso, M. Hussonnois, V. Barci, and G. Ardisson, J. Radioanal. Nucl. Chem. **153**, 293 (1991).
[8] M.C. Goffi-Kouassi, Ph.D. thesis, Université de Côte d'Ivoire, 1991.
[9] Y.A. Akovali, Nucl. Data Sheets **61**, 623 (1990).
[10] R.K. Sheline, Phys. Lett. B **205**, 11 (1988).
[11] C.F. Liang, A. Péghaire, and R.K. Sheline, Mod. Phys. Lett. A **5**, 1243 (1990).
[12] G. Ardisson, V. Barci, and O. El Samad, Phys. Rev. C **57**, 612 (1998).
[13] R. Gunnink and J.B. Nidday, Lawrence Livermore National

Laboratory Report No. UCRL-51061, 1971, 1972, Vols. I–IV.
[14] J. Gasparro, G. Ardisson, V. Barci, and J.-C. Abbé, Proceedings of the Vth Workshop on Nuclear Physics, La Habana, Cuba, 1999 [Radiochim. Acta (to be published)].
[15] R.G. Helmer, C.W. Reich, M.A. Lee, and I. Ahmad, Int. J. Appl. Radiat. Isot. **37**, 139 (1986).
[16] R.K. Sheline, C.F. Liang, and P. Paris, Phys. Rev. C **51**, 1192 (1995).
[17] J. Gasparro, G. Ardisson, V. Barci, and R.K. Sheline, Phys. Rev. C **62**, 064305 (2000), preceding paper.
[18] R.G. Helmer, M.A. Lee, C.W. Reich, and I. Ahmad, Nucl. Phys. **A474**, 77 (1987).
[19] V.G. Chumin, S.S. Eliseev, K.Y. Gromov, Y.V. Norseev, V.I. Fominyhh, and V.V. Tsupko-Sitnikov, Bull. Rus. Acad. Sci. Phys. **59**, 1854 (1995).
[20] A. Péghaire, Ph.D. thesis, Université de Paris-Sud, 1977.
[21] G. Bastin-Scoffier, C. R. Acad. Sci., Ser. B **265**, 863 (1967).
[22] B.S. Dzhelepov, R.B. Ivanov, M.A. Mikhailova, L.N. Moskvin, O.M. Nazarenko, and V.F. Rodionov, Bull. Acad. Sci. USSR, Phys. Ser. **31**, 563 (1968).
[23] T. Vylov, N.A. Golokov, B.S. Dzhelepov, R.B. Ivanov, M.A. Mikhailova, Y.V. Norseev, and V.G. Chumin, Bull. Acad. Sci. USSR, Phys. Ser. **41**, 85 (1977).
[24] R.S. Hager and E.C. Seltzer, Nucl. Data, Sect. A **4**, 1 (1968).
[25] M.A. Preston, Phys. Rev. **71**, 865 (1947).
[26] J. Kvasil, R.K. Sheline, I. Hrivnacova, C.F. Liang, and P. Paris, Int. J. Mod. Phys. E **1**, 845 (1992).